Electronic Supporting Information

Elasto-Plastic Behaviour with Reversible Thermosalient Expansion in Acrylonitrile-Based Organic Crystals

Deepak Manoharan,[a,†] Subham Ranjan,[b,†] Franziska Emmerling,[c] Biswajit Bhattacharya,[c] Satoshi Takamizawa,*[b] and Soumyajit Ghosh *[a]*

[a]Department of Chemistry, SRM Institute of Science and Technology, Kattankulathur 603 203, Tamil Nadu, India.

[b]Department of Materials System Science, Graduate School of Nanobioscience, Yokohama City University, 22-2 Seto, Kanazawa-ku, Yokohama, Kanagawa 236-0027, Japan.

[c]BAM Federal Institute for Materials Research and Testing, Richard-Willstatter-Str. 11,12489 Berlin, Germany.

† Equally contributing author

* To whom correspondence should be addressed, Email:

soumyajitghosh89@gmail.com (S.G.)

staka@yokohama-cu.ac.jp (S.T.)

biswajit.bhattacharya@bam.de (B.B.)

Materials.

4-bromo benzaldehyde, 1,4-phenylenediacetonitrile, ethanol, methanol, acetonitrile and sodium hydroxide were purchased from TCI, Sigma-Aldrich, Thermo Fischer Scientific Avra Chemicals and used as received without further purification. Analytical Research (AR) grade solvents were used for synthesis and crystallization.
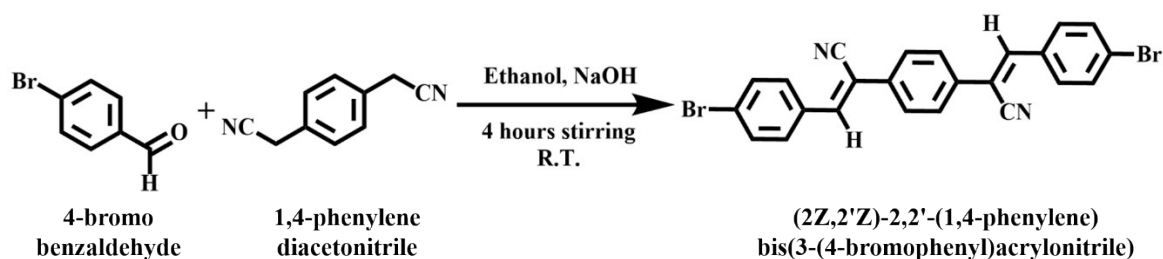

Fig. S1 Synthesis scheme of **DSBr** crystal.

Nuclear Magnetic Resonance Spectroscopy (NMR).

^{1}H-NMR spectra were recorded using a Bruker Avance III-500MHz instrument using CDCl$_3$ as a solvent for **DSBr**. ^{1}H NMR spectra were collected under standard conditions. Chemical shifts were reported in Parts per million (ppm) and referenced to the residual solvent peak at 7.26 ppm for CDCl$_3$ solvent.
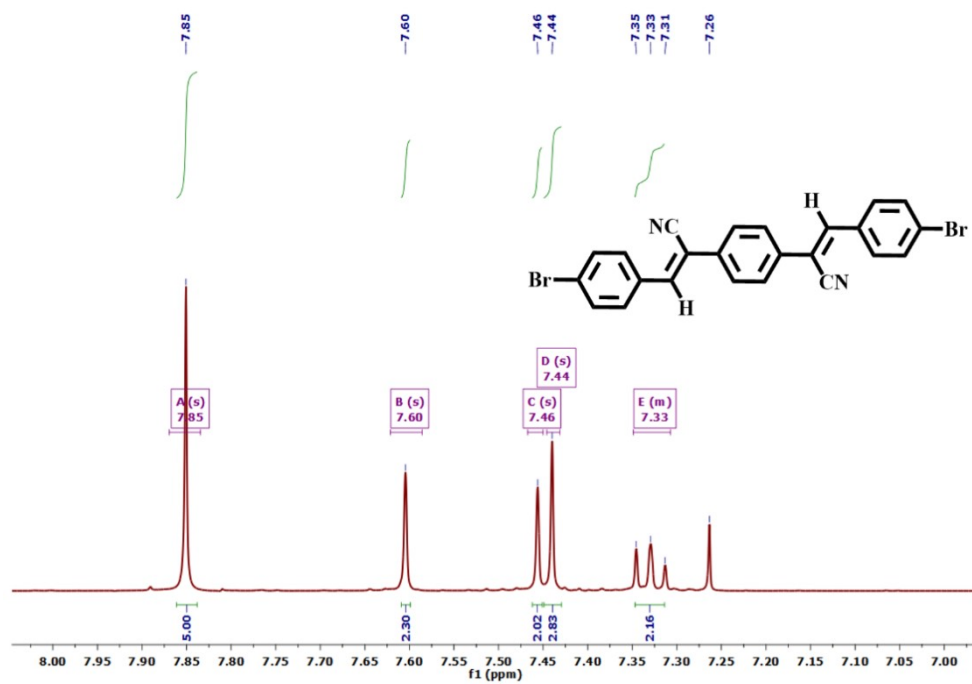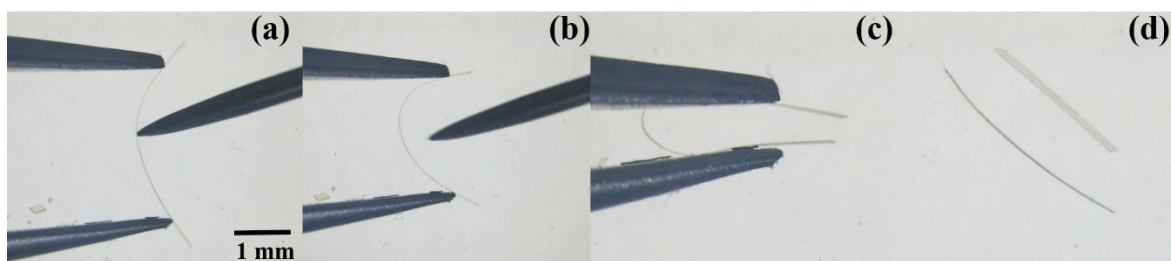
Fig. S2 ^{1}H NMR spectrum of **DSBr** crystal.

^{1}H NMR (500 MHz, CDCl$_3$) δ 7.85 (s, 5H), 7.60 (s, 2H), 7.46 (s, 2H), 7.44 (s, 3H), 7.35 – 7.31 (m, 2H).

Table S1. Crystallographic information table.

Compound	Crystal DSBr	Crystal DSBr	Crystal DSBr
Formula	$C_{24}H_{14}Br_2N_2$	$C_{24}H_{14}Br_2N_2$	$C_{24}H_{14}Br_2N_2$
Molecular weight	490.19	490.19	490.19
T/K	152	293	473
Crystal system	Triclinic	Triclinic	Triclinic
Space group	$P\bar{1}$	$P\bar{1}$	$P\bar{1}$
a/Å	3.8937 (2)	3.9746(4)	4.113(2)
b/Å	5.8230 (4)	5.8533(7)	5.888(4)
c/Å	21.4091(12)	21.594(2)	21.884(12)
α/º	88.194 (2)	92.010(4)	93.27(2)
β/º	84.820 (2)	94.227(4)	92.161(19)
γ/º	88.194 (2)	93.104(4)	94.32(2)
Volume/Å^3	482.82 (5)	499.89(9)	527.1(5)
Z	1	1	1
ρ, Mg.cm^{-3}	1.686	1.628	1.544
μ /mm^{-1}	4.209	4.066	3.856
Reflections collected	12660	3865	1362
Independent Reflections	2030	1737	676
R_{int}	0.0470	0.0376	0.0462
GOF	1.174	1.044	1.043
R1	0.0373	0.0485	0.0779
wR_2	0.0866	0.1102	0.2799
CCDC Number	2293844	2301265	2301266

Fig. S3 Stepwise elastic bending images of **DSBr** crystal.
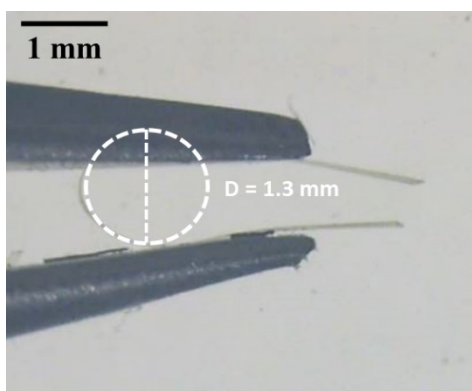
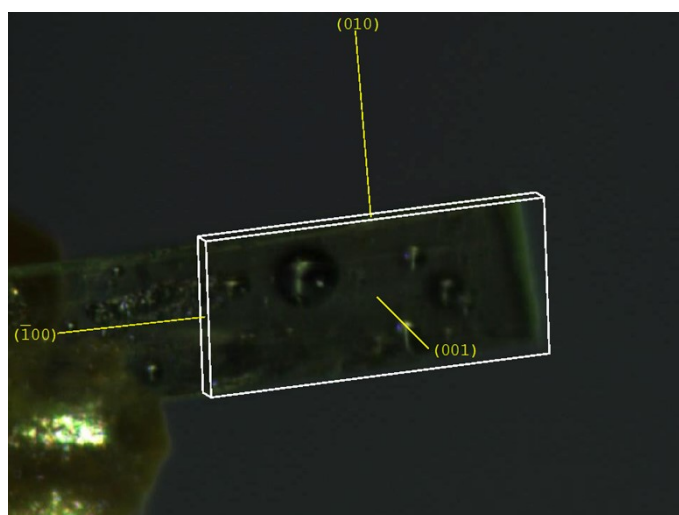**Fig. S4** Elastic strain calculation of **DSBr** crystal.

$$R = \frac{D}{2} = \textbf{0.65 mm}$$ (where D is the diameter of the semicircle formed and so radius is $\frac{D}{2}$

For a beam with thickness t,

$$\varepsilon\,(\%) = \frac{t}{2R} = \frac{0.055}{1.3} \times 100 = \textbf{4.23 \%}$$

Where '$\varepsilon\,(\%)$' is the elastic strain of the crystal, 't' is the thickness of the crystal and 'R' is the radius of the semicircle formed by bending the crystal.
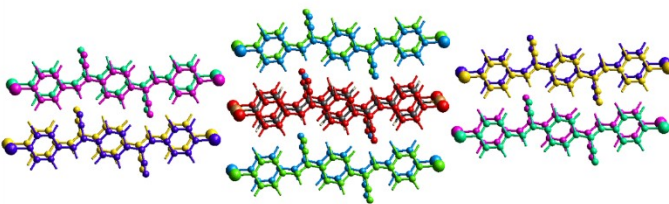

Fig. S5 Face-indexing image of **DSBr** crystal.

Energy Framework Calculations. The energy framework calculations[1,2] relating to intermolecular interactions of **DSBr** were performed using the software suite Crystal-

Explorer based on B3LYP/DGDZVP molecular wavefunctions calculated using the CIF files. For calculations, the hydrogen atoms were normalized to standard neutron diffraction values. The energy frameworks constructed were based on the crystal symmetry and total interaction energy components of which included electrostatic, polarization, dispersion and exchange repulsion components scaled by 1.057, 0.740, 0.871 and 0.618, respectively. The interaction energies below 5 kJ.mol^{-1} are omitted for clarity and the cylinder thickness is proportional to the intermolecular interaction energies along the parallel vector passing through the cylinder.

Table S2. Molecular structure pairs and the interaction energies (kJ.mol^{-1}) obtained from energy frameworks calculation for **DSBr**. Scale factors are in the lower table.
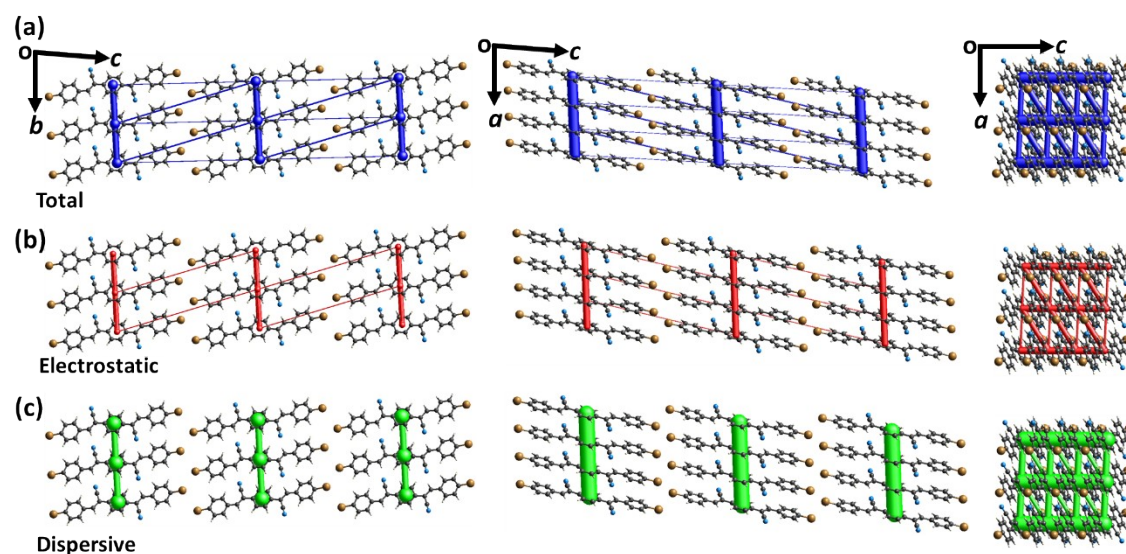

Interaction Energies (kJ/mol)
R is the distance between molecular centroids (mean atomic position) in Å.

Total energies, only reported for two benchmarked energy models, are the sum of the four energy components, scaled appropriately (see the scale factor table below)

	N	Symop	R	Electron Density	E_ele	E_pol	E_dis	E_rep	E_tot
	2	x, y, z	3.89	B3LYP/DGDZVP	-46.0	-2.9	-127.2	133.8	-78.9
	2	x, y, z	22.77	B3LYP/DGDZVP	-6.6	-0.0	-4.9	0.0	-11.2
	2	x, y, z	6.87	B3LYP/DGDZVP	-38.3	-11.2	-34.3	49.9	-47.8
	2	x, y, z	22.11	B3LYP/DGDZVP	-1.2	-0.0	-5.0	0.0	-5.6
	2	x, y, z	5.82	B3LYP/DGDZVP	-13.3	-5.2	-53.2	41.9	-38.4
	2	x, y, z	22.05	B3LYP/DGDZVP	-0.4	-0.1	-5.2	0.0	-5.0
	2	x, y, z	21.41	B3LYP/DGDZVP	1.3	-0.0	-3.8	0.0	-1.9

Scale factors for benchmarked energy models
See Mackenzie et al. IUCrJ (2017)

| Energy Model	k_ele	k_pol	k_disp	k_rep
CE-HF … HF/3-21G electron densities	1.019	0.651	0.901	0.811
CE-B3LYP … B3LYP/6-31G(d,p) electron densities	1.057	0.740	0.871	0.618

Fig. S6 Visualization of energy frameworks showing total interaction energy (a, blue); electrostatic (b, red) and dispersion (c, green) components for **DSBr**, in the (left) (100); (middle) (010) and (right) (010) faces, respectively. The energy scale factor is 100 and the energy threshold is 5 kJ.mol^{-1}.

Three-Point Bending Tests. Light-dependent three-point bending test experiments were performed using a universal testing machine coupled with polarized white light and UV light (365 nm). A single crystal on two-point support was applied stress with a metal-blade jig (Fig. S7). At a displacement rate of 2 m sec^{-1}, the jig pushed the crystal face $(001/00\bar{1})$ downward (press). The tension was released after bending, and the deformation behavior was observed using a polarized microscope. The displacement to the applied force gave the elastic moduli according to the following equation to convert it to stress and strain (mm): L is the support span (mm) and D is the center deflection.

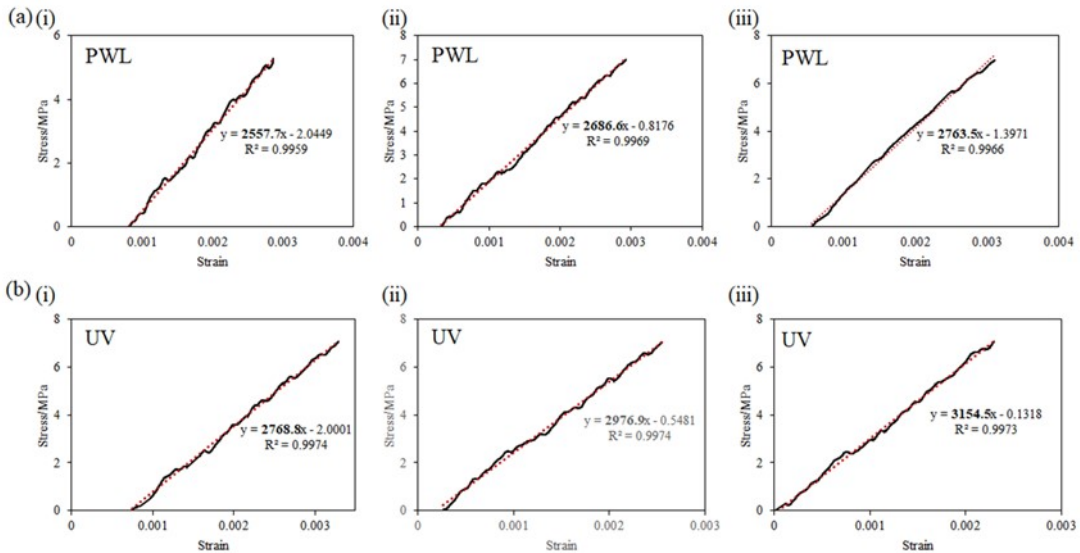$$\text{Stress} = \frac{3 \times \text{Force} \times \text{L}}{2 \times \text{width} \times \text{height}^2} \quad \cdots\cdots\cdots \quad \text{S1}$$

$$\text{Strain} = \frac{6 \times \text{D} \times \text{height}}{\text{L}^2} \quad \cdots\cdots\cdots \quad \text{S2}$$

$$\text{Elastic Modulus} = \frac{\text{Stress}}{\text{Strain}}$$
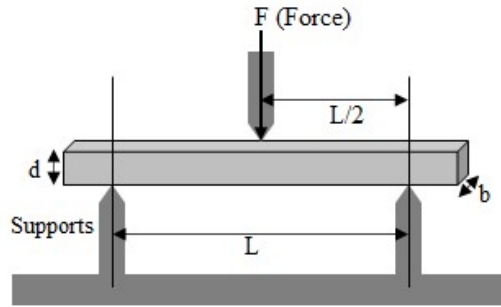
F = Force (N)
L = Support span (mm)
b = width (mm)
d = height (mm)

Fig. S7 Experimental setup of three-point bending test.
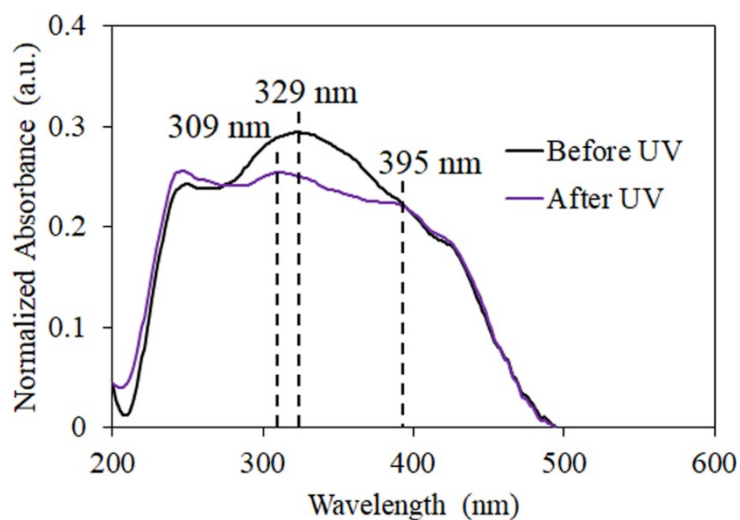

Fig. S8 Stress-strain curves of **DSBr** crystals during the three-point bending test, (a) under polarized white light (PWL) and (b) UV light. The slope of stress-strain graphs gives the calculated elastic moduli. of crystal **DSBr.**

UV-visible Spectroscopy Study

The solid-state UV-vis spectra were recorded with JASCO J-820 instrument.


Fig. S9 UV-visible spectrum of Crystal **DSBr.**

Fluorescence Microscopy Study.

The typical crystals of **DSBr** were observed under LEICA DM6B fluorescence microscope to capture optical fluorescence images. This was done with different ranges of excitation wavelengths and found to be fluorescent as shown in Figure S12.
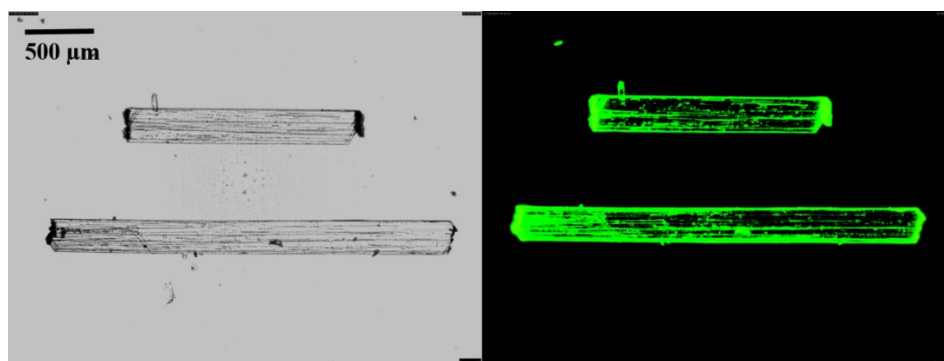
Fig. S10 Fluorescence microscopy image of Crystal **DSBr** (a) in Brightfield (b) 342-378 nm.
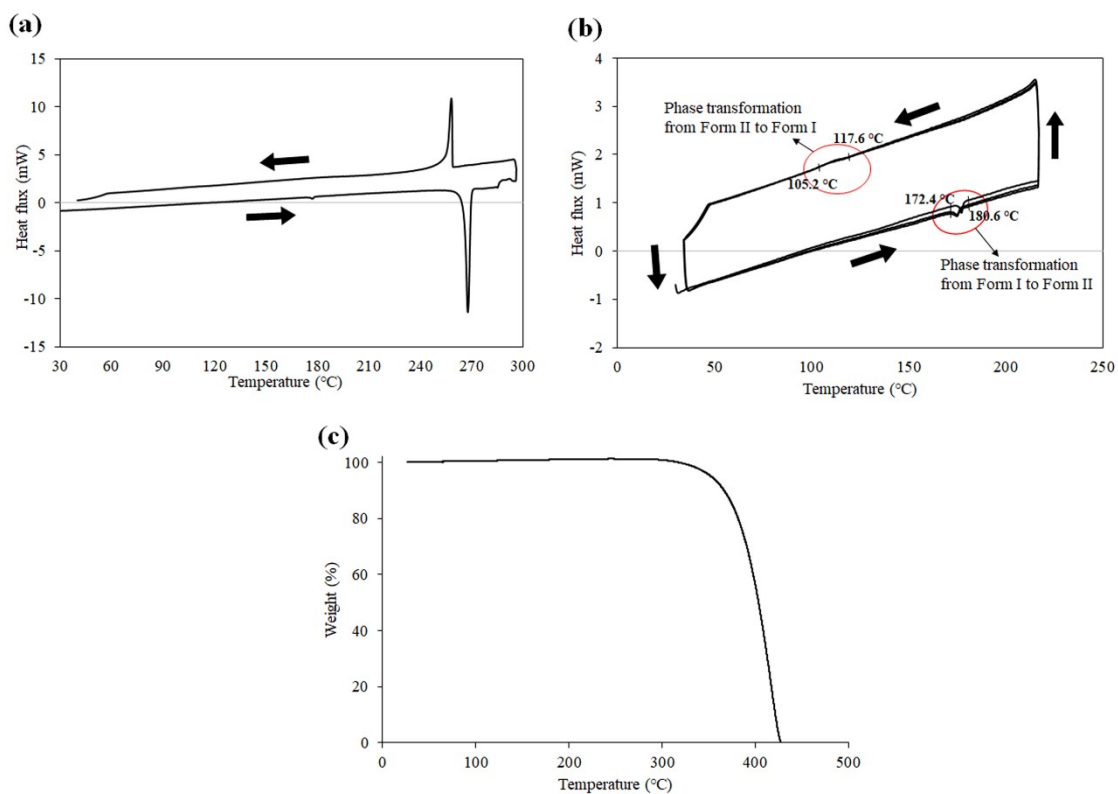
Fig. S11 DSC and TGA profile of **DSBr** gently grounded crystals. (a) Till melting; (b) phase change during three consecutive heating-cooling cycles; (c) TG profile.
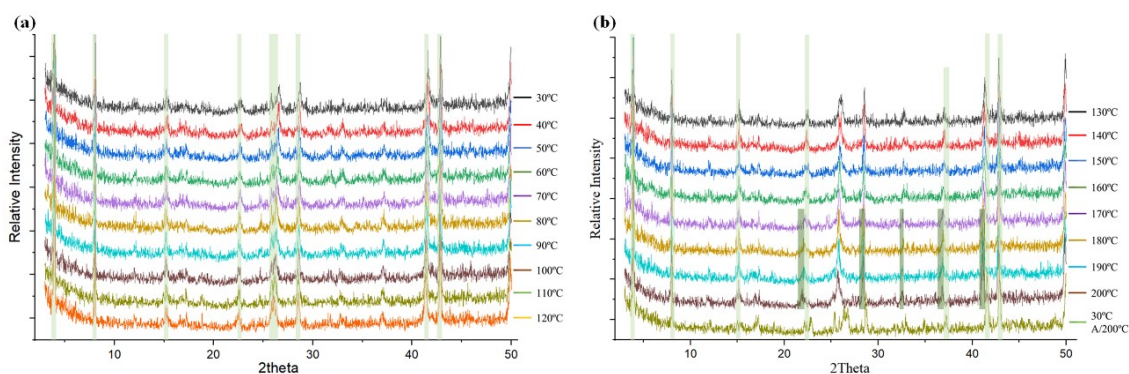
Fig. S12 Variable-temperature powder X-ray diffraction patterns of **DSBr** exhibiting a reversible phase transformation measured from 30 ºC to 200 ºC (left to right), followed by cooling to 30 ºC.

**Table S3**. Temperature changes in cell parameters obtained by single crystal X-ray diffraction analysis.

| TEMPERATURE (°C)	a	b	c	α	β	γ	Cell volume
20 °C	3.9746 (4)	5.8533 (7)	21.594 (2)	92.010 (4)	94.227 (4)	93.104 (4)	499.89 (10)
40 °C	3.9865 (5)	5.8559 (7)	21.614 (3)	92.110(4)	94.078(4)	93.219(4)	502.08 (10)
60 °C	4.0007 (5)	5.8600 (8)	21.644 (3)	92.218(5)	93.914(5)	93.335(5)	504.92 (12)
80 °C	4.0147 (6)	5.8629 (10)	21.672 (3)	92.340(6)	93.741(5)	93.454(6)	507.58 (14)
100 °C	4.026 (3)	5.863 (4)	21.733 (14)	92.60(2)	93.38(2)	93.57(2)	510.5 (6)
120 °C	4.046 (2)	5.874 (4)	21.788 (13)	92.73(2)	93.19(2)	93.72(2)	515.3 (5)
200 °C	4.113 (2)	5.888 (4)	21.884 (12)	93.27(2)	92.161(19)	94.32(2)	527.1(5)
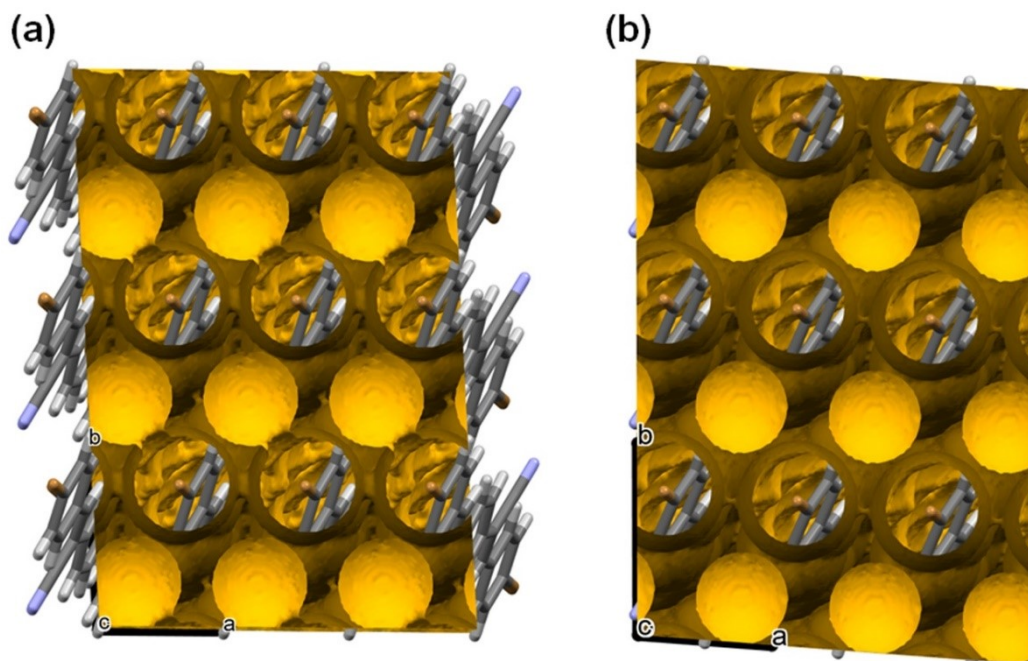
Fig. S13 Void surface view of Form I (a) and Form II (b).

Table S4: Void volume per unit cell (Å³) and porosity (%) in Form I and II.

S.No.	Volume (Å³)	% Empty space of unit cell volume
Form I	152.73	30.6
Form II	182.87	34.7
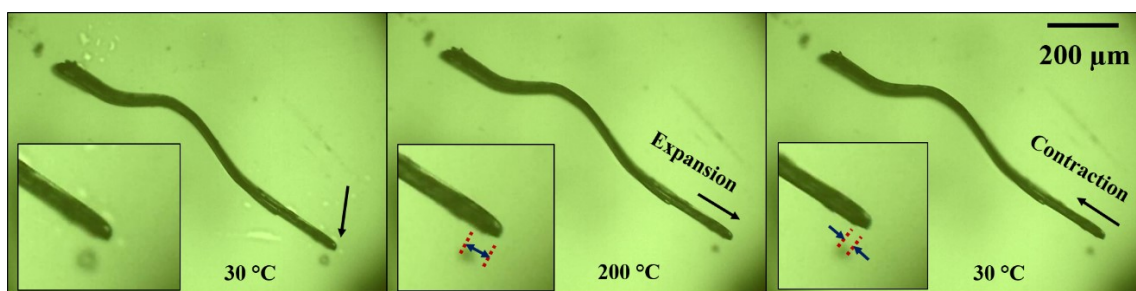
Fig. S14 Thermosalient expansion and reversible contraction of plastically bent crystal of **DSBr**.
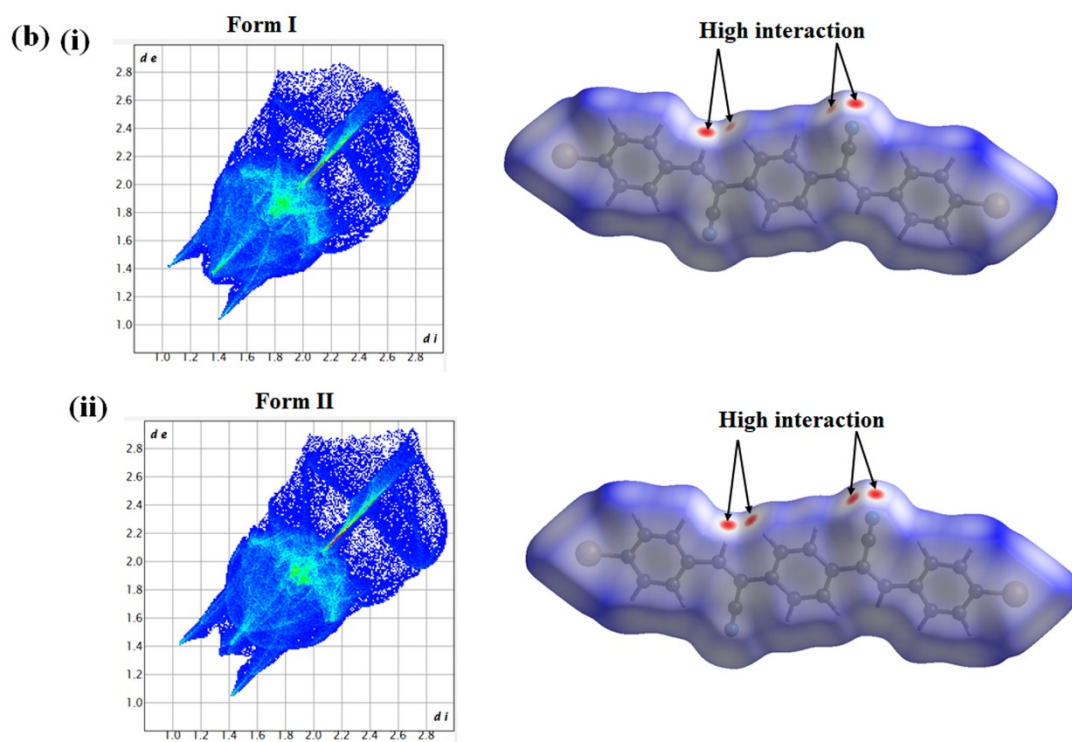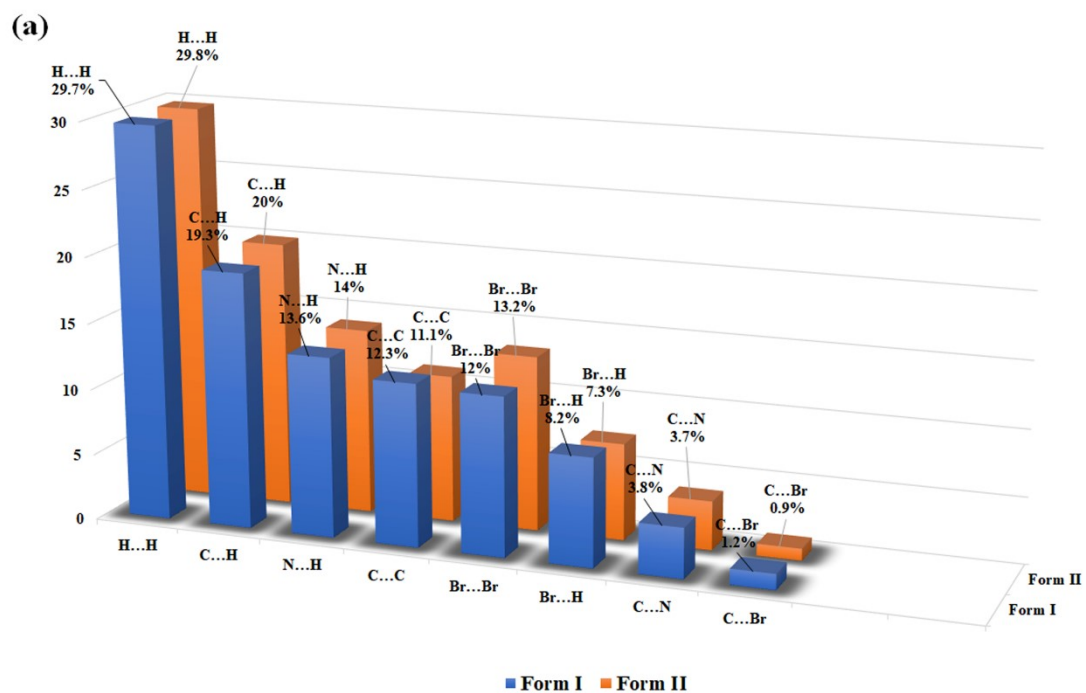
Fig. S15 The relative contribution of intermolecular interactions to the Hirshfeld surface area (a) intermolecular interactions of Form I and Form II, and (b) fingerprint plots of Form I and Form II.

References

(1) M. J. Turner, S. P. Thomas, M. W. Shi, D. Jayatilaka and M. A. Spackman, *Chem. Commun.*, 2015, **51**, 3735–3738.

(2) P. R. Spackman, M. J. Turner, J. J. McKinnon, S. K. Wolff, D. J. Grimwood, D. Jayatilaka and M. A. Spackman, *J. Appl. Crystallogr.*, 2021, **54**, 1006–1011.